

between those of cyclohexane and decalin. The value of  $[\eta]$  for P4M1P in this solvent has been shown<sup>6</sup> to be constant between 60 and 90 °C and then diminish over a 15 °C temperature interval from 6.1 to 3.0 dL g<sup>-1</sup> near the value in decalin at 135 °C. X-ray patterns are currently being obtained on P4M1P gels in cyclooctane to compare the information drawn from dilute- and concentrated-solution techniques.

The above results in which the solvent can have an influence in determining the polymer conformation not only in solution but in the dried state are similar to what has been found recently on solutions and gels of isotactic polystyrene in decalin.<sup>19</sup> The general character of this solvent effect is worth examining on other polymer solvent systems.

**Acknowledgment.** We thank Dr. F. D. Rochon of the chemistry department of the University of Quebec for advice in X-ray measurements and the Natural Sciences and Engineering Research Council of Canada (NSERC) for financial assistance.

**Note Added in Proof.** Several papers relating Japanese work on another modification<sup>20a-c</sup> of P4M1P escaped our attention during preparation of the present article. In a later publication,<sup>20d</sup> a revised version of the present comment of the Karasz, Bair, and O'Reilly work and a reindexation of the modifications anterior to the present one will be made.

## References and Notes

- (1) Tani, S.; Hamada, F.; Nakajima, A. *Polym. J.* **1973**, *5*, 86.
- (2) Hoffman, A. S.; Frier, B. A.; Condit, P. C. *J. Polym. Sci.* **1963**, *4*, 109.
- (3) Neuenschwander, P.; Pino, P. *Makromol. Chem.* **1980**, *181*, 737.
- (4) Charlet, G.; Delmas, G.; Dong, D. H., submitted for publication.
- (5) Wilkes, C. E.; Lehr, M. H. *J. Macromol. Sci., Phys.* **1973**, *B7*, 2, 225.
- (6) Dong, D. H. M.Sc. Thesis, Université du Québec, Montréal, 1980.
- (7) Jain, P. C.; Wunderlich, B.; Chanbey, D. R. *J. Polym. Sci., Polym. Phys. Ed.* **1977**, *15*, 2271.
- (8) Phuong-Nguyen, H.; Delmas, G. *Macromolecules* **1979**, *12*, 740, 746.
- (9) Stöfer, H.; Elias, H. G. *Makromol. Chem.* **1972**, *157*, 245.
- (10) Frank, F. C.; Keller, A.; O'Connor, A. *Philos. Mag.* **1959**, *4*, 200.
- (11) Litt, M. *J. Polym. Sci., Part A* **1963**, *1*, 2219.
- (12) Bassi, I. W.; Bonsignori, O.; Lorenzi, C. P.; Pino, P.; Corradini, P.; Temussi, P. A. *J. Polym. Sci., Part A-2* **1971**, *9*, 193.
- (13) Khoury, F.; Barnes, J. D. *J. Res. Natl. Bur. Stand. U.S.A.* **1972**, *76A*, 225.
- (14) Kusanagi, H.; Takase, M.; Chatani, Y.; Tadokoro, H. *J. Polym. Sci., Polym. Phys. Ed.* **1978**, *16*, 131.
- (15) Hasegawa, R.; Tanabe, Y.; Kobayashi, M.; Tadokoro, H.; Sawakura, A.; Kawai, N. *J. Polym. Sci., Part A-2* **1970**, *8*, 1073.
- (16) Benedetti, E.; Bonsignori, D.; Chellini, E.; Pino, P. *Journ. Calorim. Anal. Therm., Prepr.* **1978**, *9A*, 139, 65-71.
- (17) Natta, G.; Allegra, G.; Bassi, I. W.; Carlini, C.; Chiellini, E.; Montagnoli, G. *Macromolecules* **1969**, *2*, 311.
- (18) Karasz, F. E.; Bair, H. E.; O'Reilly, J. M. *Polymer* **1967**, *8*, 577.
- (19) (a) Girolamo, M.; Keller, A.; Miyasaka, K.; Overbergh, N. *J. Polym. Sci., Polym. Phys. Ed.* **1976**, *14*, 39. (b) Atkins, E. D. T.; Isaac, D. H.; Keller, A.; Miyasaka, K. *Ibid.* **1977**, *25*, 211. (c) Atkins, E. D. T.; Isaac, D. H.; Keller, A. *Ibid.* **1980**, *18*, 71. (d) Atkins, E. D. T.; Keller, A. *IUPAC Int. Symp. Macromolecules*, Florence, 1980.
- (20) (a) Nakajima, A.; Hayashi, S.; Taka, T.; Utsumi, N. *Kolloid Z. Z. Polym.* **1969**, *234*, 1097. (b) Tanda, Y.; Imada, K.; Takayanagi, M. *Kogyo Kagaku Zasshi* **1966**, *69*, 1971. (c) Tanda, Y.; Kawasaki, N.; Imada, K.; Takayanagi, M. *Rep. Prog. Polym. Phys. Jpn.* **1966**, *165*, 9. (d) Revol, J. F.; Charlet, G.; Delmas, G., submitted for publication.

## Crystalline Morphology of Isothermally Crystallized Branched Polyethylene

M. Glotin and L. Mandelkern\*

Department of Chemistry and Institute of Molecular Biophysics, Florida State University, Tallahassee, Florida 32306. Received March 24, 1981

**ABSTRACT:** The crystalline morphology, or supermolecular structure, of well-characterized whole polymers and fractions of branched polyethylene was systematically studied as a consequence of and during isothermal crystallization. Small-angle laser light scattering was the principal technique used, and this work necessitated a delineation of the isothermal crystallization range and a careful preliminary study of the overall crystallization kinetics under these conditions. Molecular weight, molecular weight distribution, and branching content were the principal constitutional variables investigated. Although both whole polymers and fractions respond in a similar manner to these variables, the whole polymers display a greater propensity to form spherulites after isothermal crystallization and cooling. Molecular weight fractionation is ruled out from being of any significance here, and the effect is attributed to the accessible crystallization range. Major control of spherulitic structure and size observed at room temperature can be obtained from both the extent of crystallization and the morphological form developed at the isothermal crystallization temperature. Under favorable conditions the latter can lead to "macronuclei" for spherulite formation.

## Introduction

We have previously reported studies of the crystalline morphology of isothermally crystallized molecular weight fractions of linear polyethylene as well as the rapid non-isothermal crystallization of both linear and branched fractions and whole polymers.<sup>1-4</sup> Small-angle light scattering (SALS) was the principal technique used, augmented when necessary by optical and electron microscopy. For similar crystallization conditions it was found

that the morphology, or supermolecular structure, of the linear polyethylenes is strongly influenced by molecular weight and is also extremely sensitive to polydispersity.<sup>1,2,5</sup> Molecular weight fractions with molecular weights less than about  $2 \times 10^6$  can develop rodlike morphology under appropriate crystallization conditions, while it is also possible to establish conditions under which organized morphological forms are not observed, although the characteristic lamella crystallites are present. For

Table I  
Branching<sup>a</sup> and Molecular Weight Characteristics of Unfractionated Polyethylenes

sample	Et	Bu	Am	total SCB	long-chain branching	total branching	$M_w \times 10^{-5}$	$M_w/M_n$
a	1.4	3.6	1.1	6.1	0.9	7.0	1.48	9.6
c	4.4	4.0	2.2	10.6	2.2	12.8	3.46	18.5
e	3.6	8.3	1.0	12.9	1.6	14.5	9.46	64
f	6.0	8.5	1.3	15.8	1.2	17.0	2.6	20

<sup>a</sup> Branches per 1000 carbons; based on unique resonance assignments.

branched polyethylenes, molecular weight, molecular weight distribution, and side-group concentration were the major constitutional characteristics which determined the crystalline morphology.<sup>2,4</sup> A continuous evolution in morphological form was observed from the linear polymer to chains with increasing concentrations of side-chain branches.

The previous morphological observations were all made at ambient temperature,<sup>2,4</sup> care being taken, however, to ensure that essentially all the crystallization occurred under the prescribed conditions. The only exception was for very high molecular weight linear polyethylene fractions, where a significant amount of crystallization occurs upon cooling to room temperature subsequent to isothermal crystallization. However, it was shown for this limited situation that no change in morphological form occurred upon cooling. It was previously pointed out that isothermally crystallized branched polyethylene would have to be studied differently because of the copolymeric character of its crystallization behavior.<sup>6,7</sup> The isothermal crystallization of branched polyethylene is very protracted; the relatively small amount of crystallinity that is formed isothermally develops over many decades of time. The isotherm shapes are very sensitive to the crystallization temperature under these conditions. Consequently, an appreciable amount of crystallinity develops on cooling. This effect could conceivably influence the morphology observed at ambient temperature. In fact, as will be developed subsequently, it is precisely this phenomenon which caused apparent anomalies in the previous work with isothermally crystallized, low-density (branched) polyethylene.<sup>2</sup> These factors require that the isothermally crystallized, branched samples, as well as ethylene copolymers, be studied and treated differently.

There are then the central questions of the influence of the amount of crystallinity, as well as the morphological form that develops isothermally, on the resulting structures that develop on cooling. For this type of polymer and crystallization mode, most of the crystallinity observed at room temperature occurs on cooling. Therefore these matters have to be carefully assessed and represent the main questions addressed in this paper. To properly study this problem it is necessary to first establish the isothermal crystallization range for each sample. Within the isothermal region, the extent of crystallization as a function of time and temperature and the concomitant morphology need to be determined. As a reference point for the analysis of the branched polymers, similar experiments need to be carried out with linear analogues to ascertain the effect of interrupting the crystallization process at different levels and morphologies.

## Experimental Section

**Samples.** The polymers used here were selected from among those described previously in the study of rapid nonisothermal crystallization of polyethylene. These include commercial-type high-pressure (branched) polyethylenes, molecular weight fractions of this kind,<sup>9</sup> hydrogenated polybutadienes, a linear polyethylene molecular weight fraction ( $M_w = 1.61 \times 10^5$ ), and an unfractionated

linear sample, Marlex-50, with  $M_w = 1.7 \times 10^5$  and  $M_n \approx 1.2 \times 10^4$ . The characteristics of the unfractionated, branched polymers are taken from our previous report<sup>2</sup> and are listed in Table I with the same sample designation. The properties of the branched fractions and of the hydrogenated polybutadienes are given in Table II. The latter possess a narrow molecular weight distribution with randomly distributed ethyl side groups having virtually constant co-unit composition.

**Crystallization Procedure.** To prepare a crystalline specimen for study, about 10 mg was placed between aluminum foil and pressed by a Carver press heated to about 160 °C into a film ca. 30–40- $\mu$ m thick. The thin film, still contained between the aluminum foil, was placed in a glass ampule and the assembly was heated in an oil bath at 150 °C for a least 2 h. The ampule was then rapidly transferred into another oil thermostat preset for the desired crystallization temperature. After storage in the crystallization bath for the desired time period, the glass ampule was rapidly transferred from the thermostat into a dry ice/2-propanol mixture. The sample was then removed from the aluminum foil and the desired measurements were made. Since the samples are contained in glass ampules in this work, the quenching procedure will not produce cooling rates comparable to those of the previous study,<sup>2</sup> where unconfined thin films were used. Hence differences in the morphology found between the two works will be more apparent than real.

**Small-Angle Light Scattering.** The H<sub>v</sub> SALS patterns were obtained with a photometer similar to the one described by Stein.<sup>10</sup> For the in situ crystallization studies at the elevated temperatures, the samples were placed in a specially designed hot stage maintained to  $\pm 0.5$ –1 °C. Except for specific cases cited, it can be assumed that the SALS patterns were obtained at room temperature. The theoretical basis for interpreting the light scattering patterns in terms of the crystalline morphology, or supermolecular structure, has been previously summarized. The nomenclature previously established, relating the SALS patterns to a specific crystalline morphology, will be used here.<sup>1–3</sup> Patterns labeled “a”, “b”, “c” correspond to increasingly disordered spherulites given the same letter designations. They all display the characteristic X-type patterns. Rodlike morphological forms are either designated as “d”, which also yields an X-type pattern, or are a “g” type, which gives a circularly symmetric SALS pattern. Scattering from randomly arranged lamellae, an “h”-type morphology, is limited to very low angles and is also circularly symmetric. This latter type of SALS pattern is thus not unique with respect to morphological form, and other techniques must be used to discriminate between the two cases.

**Differential Scanning Calorimetry.** The differential calorimetry measurements were carried out with a Perkin-Elmer DSC2B. The melting endotherms were obtained at scanning rates of either 10 or 20 K min<sup>-1</sup>. The measured enthalpy of fusion was converted to the degree of crystallinity,  $(1 - \lambda)_{\Delta H}$ , by taking 69 cal g<sup>-1</sup> to correspond to the enthalpy of fusion for the perfect polyethylene crystal. This calorimetric technique was also used to study the crystallization kinetics in order to determine the temperature limits for isothermal crystallization as well as the amount of crystallinity developed as a function of time at a fixed temperature.

To determine the transition from nonisothermal to isothermal crystallization, the sample was first melted in the differential calorimeter and then cooled to the desired crystallization temperature at a rate of 320 K min<sup>-1</sup>. After being held a predetermined time at this temperature, the sample was heated at a rate of 5 C min<sup>-1</sup>. The area under the endothermic peak is proportional to the amount of crystallinity developed. Crystallization kinetic isotherms can thus be established. This method is limited by

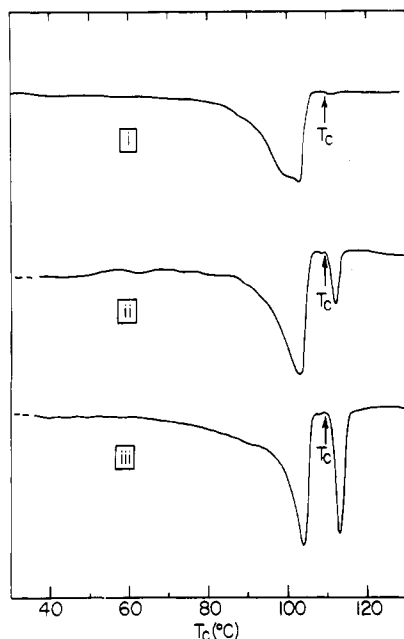


**Figure 1.** DSC curves for sample e after crystallization at 110 °C: (i) 3 h; (ii) 4 days; (iii) 12 days and subsequent quenching into dry ice/2-propanol.

practical reasons to relatively rapid crystallization processes. It was not used when crystallization took more than about 6 h. For the longer time crystallization, i.e., at higher temperatures, several films of the sample to be studied were crystallized external to the calorimeter in the manner previously described and removed from the thermostat at successive time intervals. Typical endotherms resulting from the isothermal crystallization after different time periods are given in Figure 1. It is apparent that most of these fusion curves show evidence of two distinct melting peaks. There is a very broad low-temperature peak and a sharper one at higher temperatures. The isothermal crystallization curves were constructed from these data in the following manner. The sharp peak is taken to represent melting above the crystallization temperature,  $T_c$ , while the broader one occurs at a lower temperature. In addition to their shapes, these results are definitive indication that the higher melting peak originates from those crystals formed at  $T_c$  and the lower peak corresponds to the melting of crystals formed during cooling. The change in the relative proportion of the area under the two peaks with crystallization time, at the constant temperature, supports this conclusion. Further evidence in support of this assignment is given by the results in Figure 2. Here the isothermal crystallization temperature is varied and the times appropriately adjusted. The location of the endothermic peaks above and below the crystallization temperature make the assignment clear. By converting the enthalpy of fusion of the upper peak to the degree of crystallinity at each sampling time, a crystallization kinetic isotherm can be constructed.

**Density.** The densities were obtained in an isopropyl alcohol/water gradient column at 23 °C. These values were converted to the degree of crystallinity by the relation of Chiang and Flory.<sup>11</sup>

## Results and Discussion

It is not our purpose here to analyze in detail the isothermal crystallization kinetics of these systems. They follow the broad principles involved in the crystallization kinetics of copolymers that have been established.<sup>8,12</sup> The results accentuate the difference in crystallization kinetics between homopolymers and copolymers, a fact which has not always been recognized.<sup>13</sup> For the present purposes we are only interested in the results needed to guide the morphological studies and thus only present the appropriate data. On the basis of the experimental procedures adopted here, we have arbitrarily defined the lower limit for isothermal crystallization as the temperature at which the onset of crystallization occurs after about 10 min. For

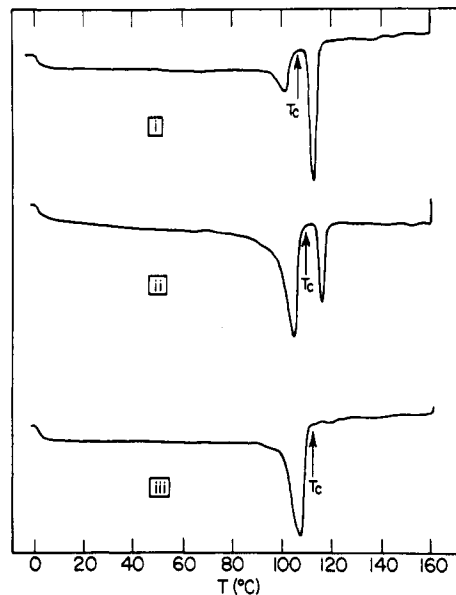


**Figure 2.** DSC curves for sample c after crystallization at (i) 106 °C for 14 days, (ii) 109 °C for 26 days, and (iii) 112 °C for 26 days and subsequent quenching into dry ice/2-propanol.

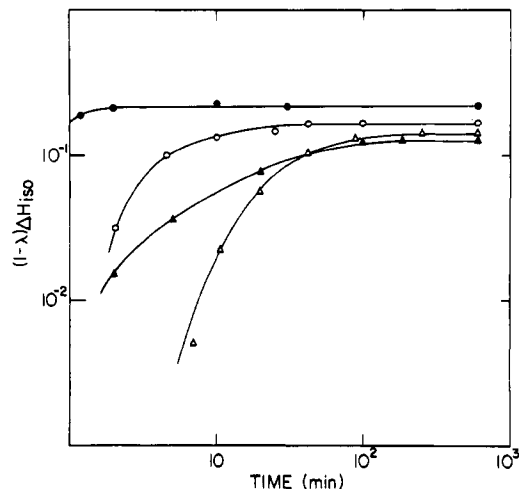


**Figure 3.** Double-logarithmic plot of degree of crystallinity against time for hydrogenated polybutadienes at 93.2 °C: (●)  $M = 16 \times 10^3$ ; (○)  $M = 1.08 \times 10^5$ ; (▲)  $M = 1.94 \times 10^5$ ; (Δ)  $M = 4.20 \times 10^5$ .

practical reasons, the highest temperature studied was set so that the total crystallization time did not exceed 30 days. Some selected crystallizations were carried out for longer time periods but did not alter the findings.

A typical set of kinetic curves obtained at 93 °C for four hydrogenated polybutadiene samples with different molecular weights, but the same co-unit content, is given in Figure 3. The early time scale of the process is strongly influenced by molecular weight, as has also been found for homopolymers.<sup>14</sup> However, the limiting value that is attained for the level of crystallinity is not nearly as dependent on molecular weight.<sup>14,15</sup> Except for the very low molecular weight sample, as has been previously reported,<sup>4</sup> the values for the copolymers do not change. They are primarily determined by the branching content.

A typical example of the temperature dependence of the crystallization kinetics is given in Figure 4 for one of the hydrogenated polybutadiene samples. Typical copolymer crystallization isotherm shapes are observed, and they cannot be superimposed upon one another.<sup>8,12</sup> As the undercooling decreases, the level of crystallinity that can

Table II  
Characteristics of Fractions of Branched Polyethylenes

sample	Me	Et	Bu	Am	total SCB	long-chain branching	total branching	$M_n \times 10^{-3}$	$M_w \times 10^{-3}$	$M_w/M_n$
A3	1.8	1.1	4.8	0.9	8.6	1.1	9.7	47.6		
A5	1.5	1.5	4.9	0.9	8.8	1.3	10.1	123		
A7	1.3	3.5	5.6	1.0	11.4	1.6	13.0	412		1.43
B4	0	4.9	9.3	0.6	14.8	0.6	15.4	10.2		1.54
B5	0	3.8	7.9	2.8	14.5	2.4	16.9	14.5		4.8
B7	0	5.4	8.0	1.2	14.6	0.8	15.4	117		16.46
B8	0	5.4	9.5	2.2	17.1	2.2	19.3	866		
B9	0							1610		
B10	0	7.3	7.1	1.2	15.6	1.0	16.6	1730		1.14
P16 <sup>a</sup>	0	21	0	0	21	0	21	16		
G25 <sup>a</sup>	0	20	0	0	20	0	20	25		
G75 <sup>a</sup>	0	18	0	0	18	0	18	75		
P108 <sup>a</sup>	0	22	0	0	22	0	22	108		1.31
P194 <sup>a</sup>	0	20	0	0	20	0	20	194		1.53
P426A <sup>a</sup>	0	22	0	0	22	0	22	413		1.84
P420 <sup>a</sup>	0	22	0	0	22	0	22	420		2.66

<sup>a</sup> Hydrogenated polybutadiene.

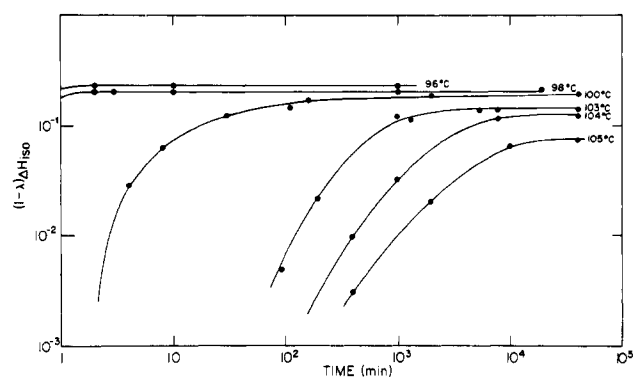


Figure 4. Double-logarithmic plot of degree of crystallinity against time for hydrogenated polybutadiene,  $M = 16 \times 10^3$ , at indicated crystallization temperatures.

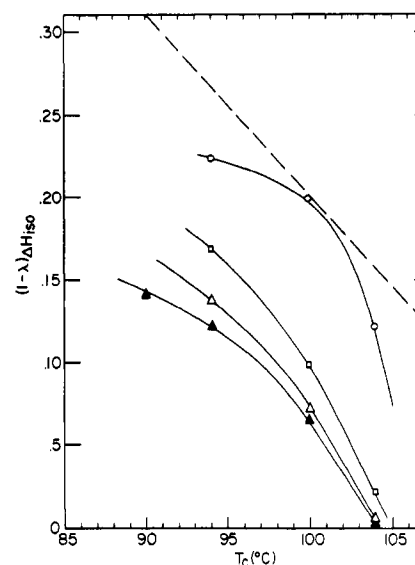


Figure 5. Maximum level of crystallinity as a function of crystallization temperature,  $T_c$ , for hydrogenated polybutadienes: (○)  $M = 16 \times 10^3$ ; (□)  $M = 1.08 \times 10^5$ ; (Δ)  $M = 1.94 \times 10^5$ ; (▲)  $M = 4.20 \times 10^5$ . Dashed line, theoretical value.

be attained significantly decreases. The crystallization kinetics are obviously quite different from those of homopolymers.

We can anticipate that the maximum level of crystallinity that can be attained at a given temperature will be important in influencing the ultimate sample morphology. As is apparent from the kinetics, this quantity will vary from sample to sample and will also be very dependent on the crystallization temperature. The maximum level of crystallinity achieved isothermally has been determined for all the samples studied. Examples of these results, demonstrating the variation with temperature, molecular weight, and branching, are shown in Figures 5 and 6. The levels of crystallinity actually attained are much less than the ideal equilibrium expectation calculated from Flory's equilibrium theory of copolymer crystallization. These values are represented by the dashed lines in the two figures.<sup>6-8</sup> The degrees of crystallinity are relatively low at the crystallization temperature. However, a significant amount of crystallinity develops upon cooling these type samples to ambient temperature. The crystallinity level then becomes essentially constant.

**Morphological Studies.** In the first set of morphological results to be presented, the SALS patterns were obtained at room temperature. Prior to cooling, the samples were maintained sufficiently long at the crystallization temperature so that the optimum amount of crystallinity

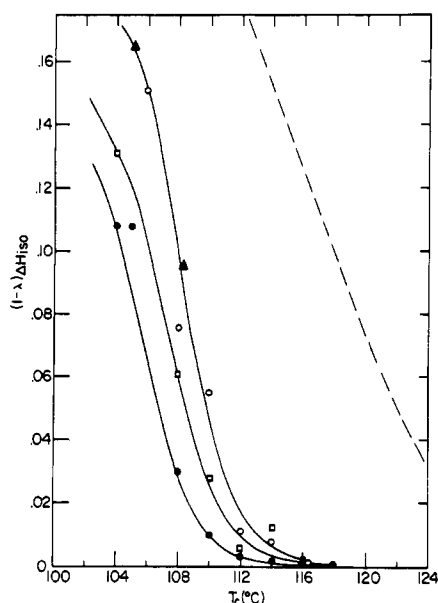


Figure 6. Maximum level of crystallinity as a function of crystallization temperature  $T_c$  for (O) unfractionated sample e and fractions ( $\blacktriangle$ ) B4, ( $\bullet$ ) B7, and ( $\square$ ) B8. Dashed line, theoretical value.

Table III  
Crystallization Conditions and Degree of Crystallinity of Unfractionated Samples

sample	isothermal crystallization		density, $a$ g cm $^{-3}$	$(1 - \lambda)_d^c$	$(1 - \lambda)_{\Delta H}^b$
	temperature, $^{\circ}\text{C}$	time, days			
a	106	7	0.9326	58.0	31.6
	109	15	0.9349	59.6	28.1
	112	15	0.9323	57.9	22.3
	114	13	0.9316	57.4	18.8
	116	26	0.9331	58.4	15.0
	118.8	30	0.9290	55.6	8.3
c	106	14	0.9195	49.2	20.8
	109	26	0.9211	50.3	6.9
	112	26	0.9173	47.7	trace
	114	50	0.9178	48.0	0
	116	50	0.9164	47.0	0
e	108	7	0.9194	49.1	7.6
	110	65	0.9207	50.0	5.5
	112	42	0.9192	48.9	1.1
	114	42	0.9192	48.9	trace
	116	42	0.9195	49.2	0

$a$  At room temperature.  $b$  At crystallization temperature.  $c$  In percent.

was developed. However, it was found that a significant portion, if not most, of the crystallinity which contributed to the light scattering pattern developed on cooling, rather than at the isothermal crystallization temperature. The magnitude of this effect can be seen from the data compiled in Table III for the whole polymers. Here the degree of crystallinity attained isothermally, given in the last column as  $(1 - \lambda)_{\Delta H}$ , can be compared with the total crystallinity,  $(1 - \lambda)_d$ , at ambient temperature. Depending on the sample and the initial crystallization temperature, the amount of crystallinity developed on cooling ranges from about half to virtually all of that observed. Thus the increase in crystallinity can be quite substantial, particularly after crystallization at the highest temperatures, where only very small amounts of crystallinity are attained.

The SALS patterns for sample e, an unfractionated, branched polyethylene crystallized at the temperatures

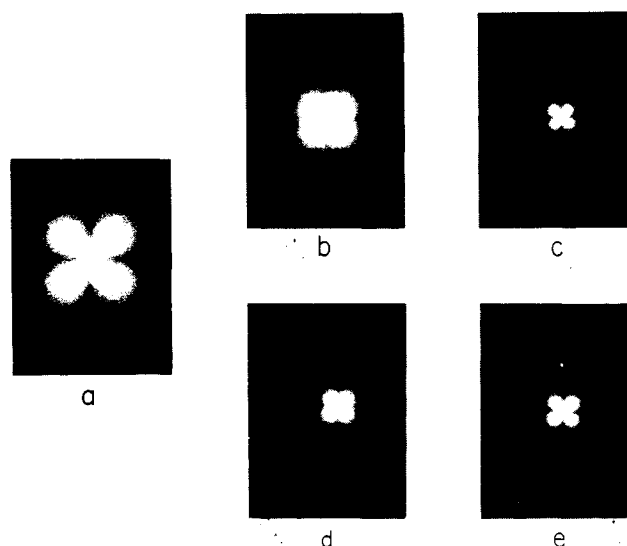
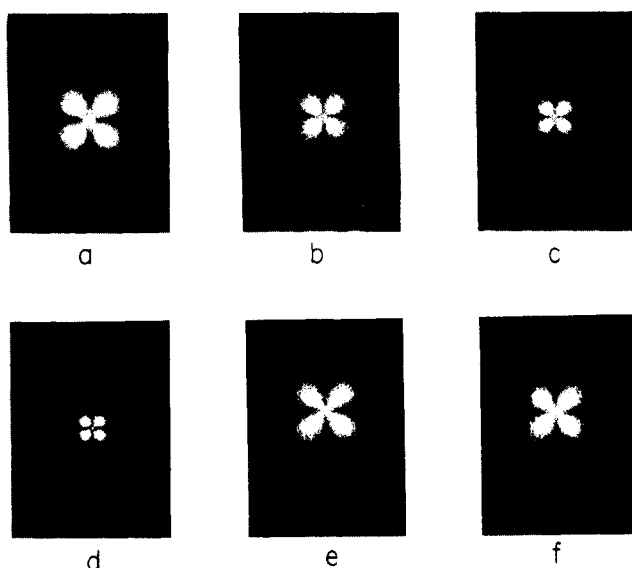


Figure 7.  $H_v$  SALS patterns for unfractionated sample e: pattern a, reference quenched into dry ice/2-propanol mixture; pattern b,  $T_c = 108^{\circ}\text{C}$ , 7 days; pattern c,  $T_c = 110^{\circ}\text{C}$ , 13 days; pattern d,  $T_c = 112^{\circ}\text{C}$ , 42 days; pattern e,  $T_c = 116^{\circ}\text{C}$ , 42 days.

indicated and cooled in the manner described above, are shown in Figure 7. A reference pattern for this sample, where no crystallinity was allowed to develop at the elevated isothermal temperature, is given for comparative purposes. The patterns for all the samples in this series represent well-defined spherulitic morphologies. No influence is evident here of the prior isothermal crystallization on the type of the supermolecular structure that results. (The SALS pattern presented here for the reference sample (quenched) is different from that reported previously for the same sample undergoing a similar thermal treatment.<sup>24</sup> This difference, however, is more apparent than real when we recall that the specimens are enclosed in glass ampoules in this work. The cooling rate is slower, and we obtain more organized crystalline morphologies here. These same comments are also applicable to the reference samples of Figures 8–10). However, it is apparent that, for this polymer, as the isothermal crystallization temperature is increased, larger size spherulites are obtained after cooling. For example, the spherulite radius, which is about  $3\ \mu\text{m}$  for the reference sample, increases to about  $9\ \mu\text{m}$  for the highest isothermal crystallization temperature. The ultimate level of crystallinity for all the initial crystallization temperatures is about the same; the amount developed isothermally increases with decreasing temperature. The designation "trace" in Table III as compared with no crystallinity is a qualitative distinction. The fact that large spherulites develop subsequent to long-time storage at  $116^{\circ}\text{C}$  is indicative of the development of some undetected crystallinity.

Qualitatively similar morphological results are found for sample c when it is subjected to a similar thermal treatment. The corresponding light scattering patterns are given in Figure 8. The lower isothermal crystallization temperatures yield spherulitic sizes which are larger than for the reference sample. Larger sizes, about  $10\ \mu\text{m}$ , are also found after isothermal crystallization at  $112^{\circ}\text{C}$ , where only a trace of crystallinity develops. However, after long-time storage at  $114$  and  $116^{\circ}\text{C}$ , the light scattering patterns are essentially identical with those for the reference with the same spherulitic radii. Consistent with the data in Table III, we can conclude that no crystallinity develops at these two temperatures for this polymer. Although sample c has a slightly smaller branching content



**Figure 8.**  $H_v$  SALS patterns for unfractionated sample c: pattern a, reference quenched into dry ice/2-propanol; pattern b,  $T_c = 106^\circ\text{C}$ , 14 days; pattern c,  $T_c = 109^\circ\text{C}$ , 26 days; pattern d,  $T_c = 112^\circ\text{C}$ , 26 days; pattern e,  $T_c = 114^\circ\text{C}$ , 50 days; pattern f,  $T_c = 116^\circ\text{C}$ , 50 days.

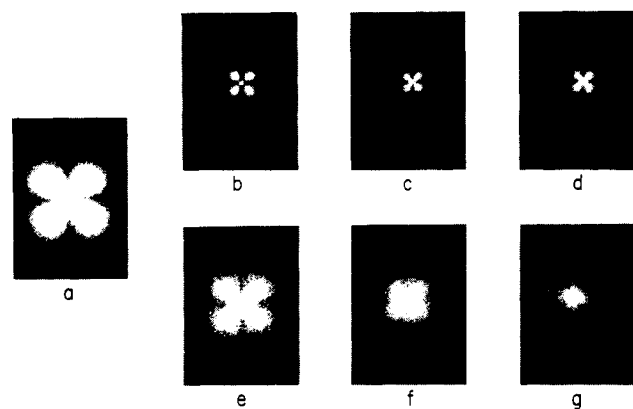


**Figure 9.**  $H_v$  SALS patterns for unfractionated sample a (sample-film distance, 98 mm except as noted): pattern a, reference quenched into dry ice/2-propanol; pattern b,  $T_c = 109^\circ\text{C}$ , 15 days; pattern c,  $T_c = 112^\circ\text{C}$ , 15 days; pattern d,  $T_c = 114^\circ\text{C}$ , 13 days; (sample-film distance, 240 mm) pattern e,  $T_c = 114^\circ\text{C}$ , 13 days (same as d); pattern f,  $T_c = 116^\circ\text{C}$ , 26 days; pattern g,  $T_c = 118.8^\circ\text{C}$ , 30 days.

than sample e, 1.28 as compared to 1.45 mol %, <sup>2</sup> crystallinity develops more readily at the elevated temperatures in the latter sample. This result could be caused by the much broader molecular weight distribution in this case.<sup>2</sup>

The main result for these two unfractionated branched polyethylene samples, namely, that spherulitic structures are always formed after isothermal crystallization and subsequent cooling, are in accord with our earlier report.<sup>2</sup> It was concluded previously that spherulite formation after isothermal crystallization was characteristic of unfractionated branched polyethylenes.<sup>2</sup> Although several different samples were studied previously, the complete temperature range and extent of isothermal crystallization were not investigated in detail. Similar morphological studies with sample a, which contains only 0.7 mol % branch groups, show some departure from this generalization. This sample is, however, approaching the molecular constitution of a linear polymer. The light scattering patterns for this case are given in Figure 9. Cooling subsequent to crystallization at the lower isothermal crystallization temperatures yields large, well-developed

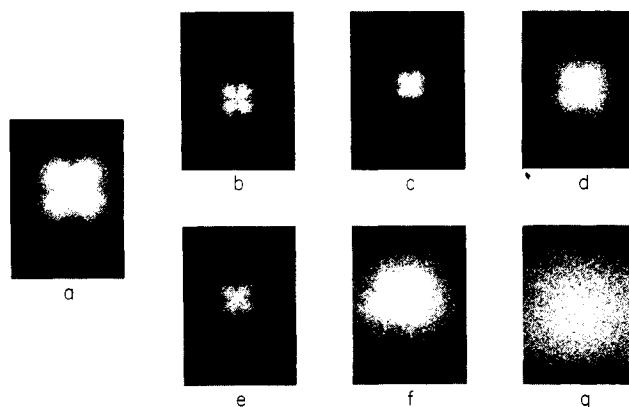


**Figure 10.**  $H_v$  SALS patterns for unfractionated linear polyethylene (Marlex-50): pattern a, reference quenched into dry ice/2-propanol; pattern b,  $T_c = 117.5^\circ\text{C}$ , 10 h; pattern c,  $T_c = 120^\circ\text{C}$ , 28 h; pattern d,  $T_c = 123.5^\circ\text{C}$ , 58 h; pattern e,  $T_c = 125.5^\circ\text{C}$ , 58 h; pattern f,  $T_c = 128^\circ\text{C}$ , 91 h; pattern g,  $T_c = 129.8^\circ\text{C}$ , 91 h.

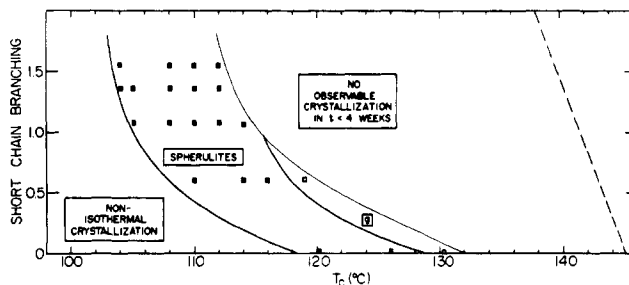


**Figure 11.** Morphological map of unfractionated, branched polyethylenes. Plot of mole fraction short-chain branching against initial isothermal crystallization temperature. Curves described in text; morphological forms as indicated in figure.

spherulites, consistent with the established morphological pattern. The reference is also spherulitic. However, when the isothermal crystallization temperature is above  $117^\circ\text{C}$ , the SALS pattern indicates that the spherulitic morphology is lost upon cooling. The pattern that is obtained at room temperature under these crystallization conditions corresponds to a "g"-type, rodlike morphology.<sup>1,3</sup> Thus for unfractionated polyethylenes, there are conditions, albeit limited ones, where a nonspherulitic morphology can be developed subsequent to isothermal crystallization.

In order to establish a reference point for the unfractionated branched polyethylenes subject to the described crystallization procedure, a linear, unfractionated sample, Marlex-50, was also studied. The pertinent SALS patterns are given in Figure 10. The results are very similar to those for the branched sample a (Figure 9). Large, well-developed spherulites are formed at the lower isothermal crystallization temperatures. The reference for this polymer is also spherulitic. However, after crystallization at the very highest isothermal temperatures, where about 60% crystallinity is attained, there is no evidence for subsequent spherulite formation. Instead there is a transition to the "g"-type morphology, which is very similar to that observed for sample a.

The results for the unfractionated polyethylenes, where the morphological form is observed at room temperature subsequent to prior complete isothermal crystallization at a predetermined temperature, are summarized in Figure 11. In this morphological map, the mole fraction of short-chain branching is plotted against the isothermal crystallization temperature prior to cooling. The temperature range of the experiments is defined by the lower and upper solid curves. These curves represent the ex-

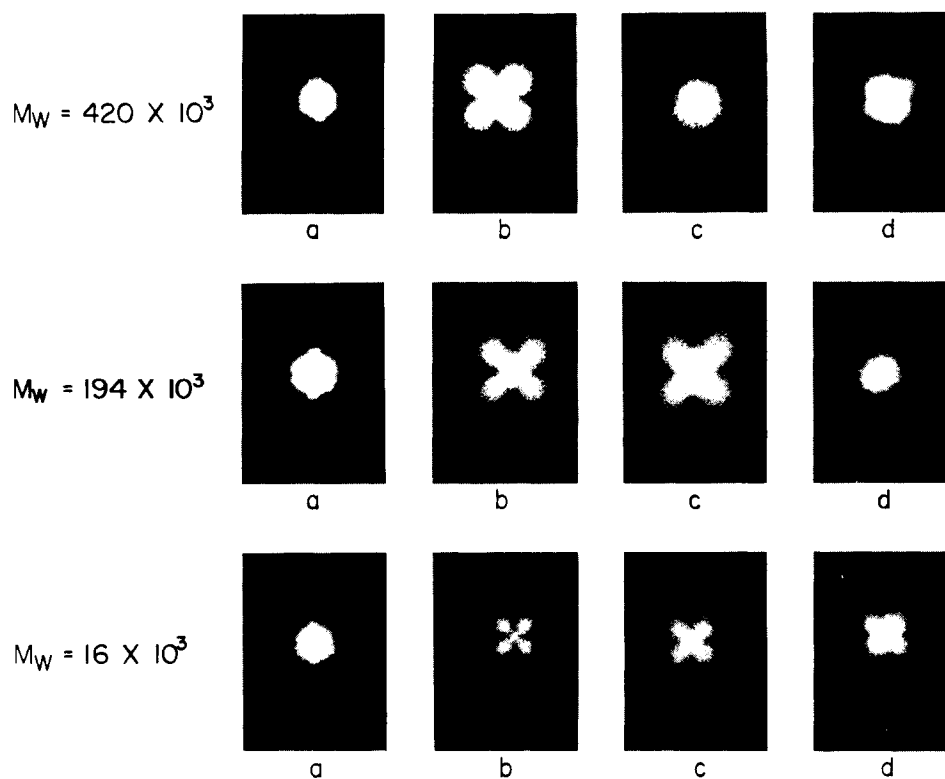


**Figure 12.**  $H_v$  SALS patterns for hydrogenated polybutadiene samples having narrow molecular weight distributions.  $M_w = 420\,000$ : pattern a, reference quenched into dry ice/2-propanol; pattern b,  $T_c = 94^\circ\text{C}$ , 8 days; pattern c,  $T_c = 100^\circ\text{C}$ , 16 days; pattern d,  $T_c = 104^\circ\text{C}$ , 28 days.  $M_w = 194\,000$ : pattern a, reference quenched into dry ice/2-propanol; pattern b,  $T_c = 94^\circ\text{C}$ , 8 days; pattern c,  $T_c = 100^\circ\text{C}$ , 28 days; pattern d,  $T_c = 104^\circ\text{C}$ , 30 days.  $M_w = 16\,000$ : pattern a, reference quenched into dry ice/2-propanol; pattern b,  $T_c = 94^\circ\text{C}$ , 3 days; pattern c,  $T_c = 100^\circ\text{C}$ , 6 days; pattern d,  $T_c = 107^\circ\text{C}$ , 28 days.

perimentally determined boundary between isothermal and nonisothermal crystallization and the temperatures at which no crystallinity could be detected after 4 weeks. The dashed line is the theoretical equilibrium melting temperature,  $T_m$ , for a random copolymer with co-unit content  $X_A$  calculated according to<sup>6,7</sup>

$$1/T_m - 1/T_m^\circ = (R/\Delta H_u) \ln X_A \quad (1)$$

The equilibrium melting temperature,  $T_m^\circ$ , was taken as  $145^\circ\text{C}$  for the present purpose<sup>16</sup> and  $\Delta H_u = 950\text{ cal/mol}$ .<sup>17</sup> For these branched polymers there is a very large temperature interval below the equilibrium melting temperature where crystallization does not occur within any reasonable time period. This interval increases substantially with increased branching content. For example, while for the linear polymer crystallization can be carried out at undercoolings of about  $15^\circ\text{C}$ , comparable rates for the highest short-chain-branched sample require undercoolings of about  $28^\circ\text{C}$ .

The reference form for all these samples, i.e., after rapid crystallization from the melt, is always found to be spherulitic. We find from Figure 11 that, except for a small region in space restricted to samples of low co-unit content and very high initial crystallization temperatures, spherulites are always observed following isothermal crystallization and cooling. Although there is no change in the morphological form, relative to the reference samples, that is developed by adopting this procedure, the spherulites that are obtained are much larger and better developed. A rodlike morphology is observed under the very limited circumstances of high crystallization temperatures and low co-unit content.

This crystallization procedure was also carried out with molecular weight fractions of branched polyethylenes. For isothermally crystallized linear fractions, nonspherulitic

morphologies are commonly observed.<sup>1</sup> Again we note (see Figures 3 and 4) that relatively small levels of crystallinity are attained isothermally for the branched fractions as compared to the linear ones. Initial studies of branched fractions crystallized at an elevated temperature prior to cooling have also been found to develop nonspherulitic morphologies.<sup>2</sup> We examine this aspect of the problem in somewhat greater detail here. The SALS patterns for a selected set of hydrogenated polybutadiene samples, each of a narrow molecular weight distribution with essentially the same co-unit content, are presented in Figure 12. This branching content is slightly higher than for those samples studied previously.<sup>2</sup> The reference for each of the molecular weights yields an "h"-type light scattering pattern corresponding to an "h"-type morphology. For the lower molecular weight fractions, as is illustrated in Figure 12, the prior crystallization at the elevated temperatures allows for a somewhat poorer type spherulite to form, in contrast to the random lamellae. The temperature interval over which this morphological change can be accomplished becomes more limited as the molecular weight increases. However, control of morphology as a consequence of the specific thermal history adopted is clearly evident in the light scattering patterns of Figure 12. A morphological map for this crystallization procedure, for the hydrogenated polybutadienes, is presented in Figure 13. The experimentally determined boundary between isothermal and nonisothermal crystallization is given in this figure as is the temperature-composition relation for which crystallization does not take place within 4 weeks. We note that as the molecular weight increases, the region over which spherulites form becomes narrower and eventually a random morphology develops at the higher molecular weights for both high and low isothermal crystallization temperatures.

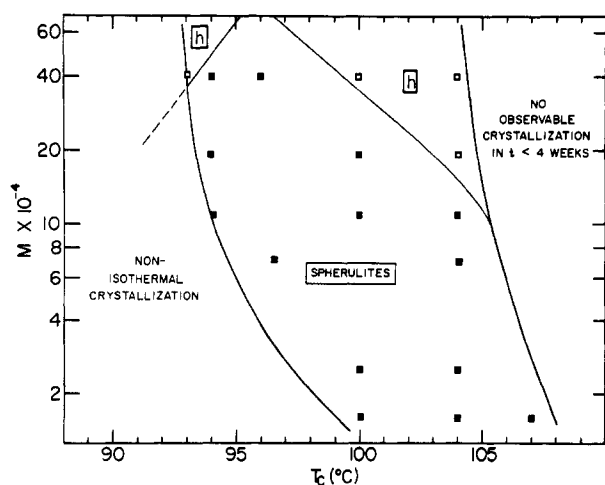


**Figure 13.** Morphological map for hydrogenated polybutadiene fractions. Plot of weight-average molecular weight,  $M_w$ , against isothermal crystallization temperature. Curves described in text; morphological forms designated in figure.

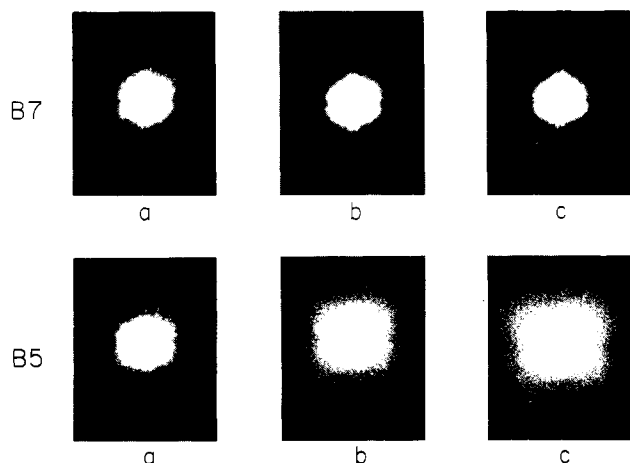


**Figure 14.**  $H_v$  SALS patterns for branched polyethylene fractions. Fraction B5,  $M_w = 14.5 \times 10^3$ : pattern a, reference sample quenched into dry ice/2-propanol mixture; pattern b,  $T_c = 105^\circ\text{C}$ , 7 days; pattern c,  $T_c = 114^\circ\text{C}$ , 45 days. Fraction B7,  $M_w = 1.17 \times 10^6$ : pattern a, reference sample quenched into dry ice/2-propanol mixture; pattern b,  $T_c = 105^\circ\text{C}$ , 7 days; pattern c,  $T_c = 116^\circ\text{C}$ , 60 days.

For other branched polyethylene fractions of the type described in Table II, it is found that after complete isothermal crystallization and subsequent cooling, the morphology for the lower molecular weights is either random lamellae or "g"-type rods. The references are again random lamellae. Typical SALS patterns for samples B5 and B7,  $M_w = 14.5 \times 10^3$  and  $117 \times 10^3$ , respectively, are shown in Figure 14. Spherulitic structures are clearly not developed in these cases. The morphological interpretation of the SALS patterns has been confirmed by thin-section transmission electron microscopy.<sup>4</sup>

It is possible to select a set of fractions from among those studied where the molecular weights are very similar but the branching content varies. A morphological map can then be constructed similar to that for the whole polymers (Figure 11). Here the variables are the branching concentration and initial isothermal crystallization temperature. For illustrative purposes we have selected the properties of samples P108 ( $M_w = 108000$ ), B7 ( $M_w = 117000$ ), A5 ( $M_w = 123000$ ), and a linear fraction of comparable molecular weight. Thus although the molecular weights are similar the short-chain branching concentration varies from 0 to 2 mol %. The corresponding morpho-

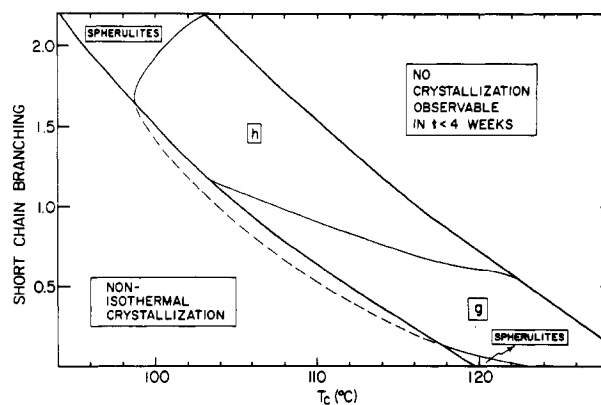


**Figure 15.** Morphological map for fractions of approximately the same molecular weight but varying branching content. Plot of branching concentration against isothermal crystallization temperature. Regions for morphological forms designated in figure.

logical map is given in Figure 15. The transition between spherulites and random lamellae in the nonisothermal crystallization region is represented by the dashed line in this figure. The 2 mol % co-unit fraction crystallizes isothermally at the lower temperatures in this plot. Despite the major structural disruption caused by this concentration of chain irregularities, spherulites are formed in accord with the data previously presented in Figure 13. As the co-unit content decreases, the range of isothermal crystallization temperatures increases, and there is a wide region where random lamellae are now formed. For fractions having the lowest co-unit content, "g"-type rods develop. Their structures are also found for the linear polymer at the higher crystallization temperatures. There is also a very small region, corresponding to the lower end of the isothermal crystallization range, where the linear polymer and, presumably, those with very low co-unit content form spherulites. A similar morphological map can also be deduced from the data available for other fractionated samples. For molecular weights greater than  $\sim 110000$  the region where spherulites are observed would be reduced compared to that shown in Figure 15. For lower molecular weights, the spherulite-forming region would be increased slightly. However, the main effect of lowering the molecular weight results in the "g"-type morphological form occurring at the expense of random lamellae.

The first phase of these morphological studies, based on the defined crystallization procedure, has shown that for both fractionated and unfractionated polyethylenes, either spherulitic or nonspherulitic structures can be obtained, depending on the sample constitution and the prior isothermal crystallization temperatures. Spherulitic structures are by far the most predominant form found with whole polymers.<sup>2</sup> Nonspherulitic structures are most frequently found with the molecular weight fractions under these crystallization conditions. Spherulitic structures can be avoided in whole polymers only under the limited conditions of very low branching and high initial isothermal crystallization temperatures. The results are thus quite different for the whole polymers and fractions although both systems are governed by similar factors. Low levels of side-chain branching and initial crystallization at very high temperatures will favor nonspherulitic structures; an increase in branching concentration or a decrease in the crystallization temperature will favor spherulite formation. We also note that random copolymers, containing 2 mol % co-units form spherulites. Morphological observation at room temperature remains, however, a very indirect way



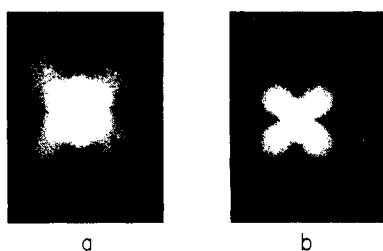


**Figure 16.**  $H_v$  SALS patterns for the isothermal crystallization of hydrogenated polybutadiene sample,  $M_w = 1.94 \times 10^5$ : pattern a, after crystallization at 95 °C and observed at this temperature; pattern b, after rapid cooling to room temperature.

of investigating the isothermally crystallized structures in the branched polyethylenes since most of the crystallinity has developed during cooling. The results presented so far give strong evidence that the isothermal crystallization temperature, and by inference the amount of crystallinity developed and possibly the high-temperature morphological form, can have a strong bearing on the results. Thus, what we have essentially discussed so far has been a description of how the morphology of a rapidly crystallized sample is modified by relatively small amounts of initial crystallinity. These results thus point out the importance of studying the isothermal crystallization morphology in situ.

We initiate the analysis of the isothermally crystallizing samples with the study of a hydrogenated polybutadiene fraction. The crystallization kinetic results, summarized in Figure 3, indicate that the levels of crystallinity that can be attained vary from 15 to 25%, depending on the molecular weight. An example of an in situ light scattering experiment is shown in Figure 16 for the hydrogenated polybutadiene sample  $M = 1.94 \times 10^5$ . Here the sample was initially heated to 150 °C for 2 h in the light scattering apparatus and then cooled to 95 °C and allowed to isothermally crystallize. The light scattering pattern shown in Figure 16a was obtained after the sample crystallized for 3 days under these conditions. The kinetic studies indicate that the level of crystallinity attained is 12–13%. With small levels of crystallinity, as in these samples, most of the light scattering originates from the amorphous portions. However, this scattering is weak and restricted to small angles so organized structures can be discerned. The SALS pattern in Figure 16a shows that even at this low level of crystallinity spherulites have developed, although they are small and highly disordered. When this sample is subsequently rapidly cooled from the hot stage, the SALS pattern of Figure 16b results. This pattern indicates a change from “c”- to a “b”-type spherulitic structure. Upon further crystallization the same morphological form continues to develop, although the spherulites have become larger and better developed. The main conclusion at this juncture is that one can distinguish morphological forms in situ with samples of low levels of crystallinity and changes in supermolecular structure can occur on cooling.

A more detailed study of a crystallizing polymer is illustrated in Figure 17 for unfractionated sample e crystallizing at 106 °C. After 52 h at this temperature, 15% crystallinity has developed. The formation of spherulitic structures at this temperature is clearly indicated by the SALS patterns. Cooling this sample improves the spherulitic order. Raising the crystallization temperature of this sample to 110 °C retards the crystallization rate and reduces the maximum amount of crystallinity developed to only 5%. The SALS patterns accompanying this crystallization are shown in Figure 18. Although these

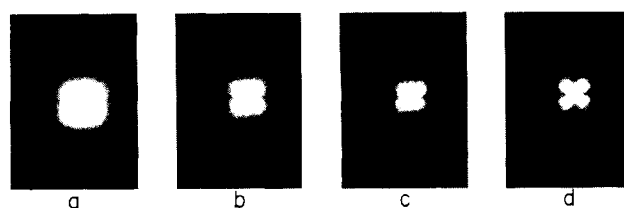


**Figure 17.**  $H_v$  SALS for the isothermal crystallization of unfractionated, branched sample e crystallizing at 106 °C: pattern a, observed at 106 °C after 4 h; pattern b, observed at 106 °C after 28 h; pattern c, observed at 106 °C after 52 h; pattern d, cooling to room temperature after 52 h at 106 °C.

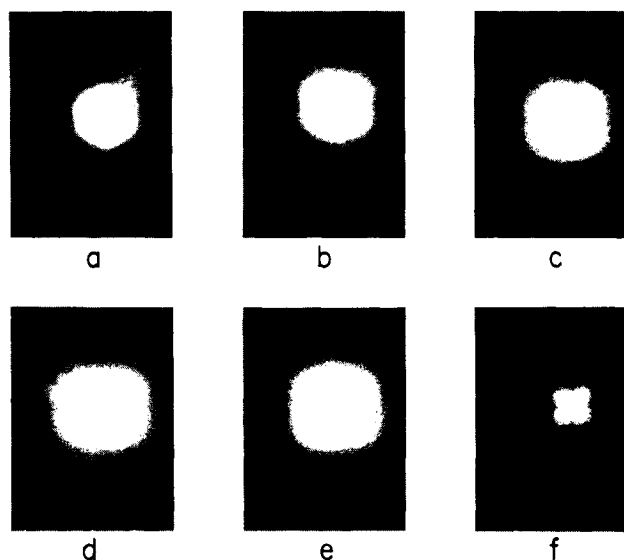


**Figure 18.**  $H_v$  SALS patterns for the isothermal crystallization of unfractionated branched sample e crystallizing at 110 °C: pattern a, initial sample observed at 110 °C; pattern b, observed at 110 °C after 2 days; pattern c, observed at 110 °C after 4 days; pattern d, observed at 110 °C after 6 days; pattern e, observed at 110 °C after 9 days; pattern f, crystallized at 110 °C for 10 days and rapidly cooled to room temperature.

patterns are difficult to interpret in detail, there is clear indication of an azimuthal dependence to the scattering and the development of fourfold symmetry. It is not possible, however, to distinguish the specific crystalline morphology. However, when after crystallizing for 10 days at this temperature this sample is rapidly cooled to room temperature, relatively large spherulites are formed. These structures are deduced from the last SALS pattern in the series and the spherulites are approximately 10–15  $\mu\text{m}$  in diameter. An examination of this sample in the polarized light microscope at room temperature revealed that the spherulites formed have a narrow size distribution. This observation, together with the large spherulitic size, indicates that the crystallization at this high temperature did not result in the growth of a few large spherulites followed on cooling by the nucleation and growth of smaller ones. These data suggest instead that a small number of “seeds” or “spherulitic nuclei” are formed at the elevated temperature which then act as centers for the further growth of spherulites upon cooling.

A comparative study was carried out with fraction B7, which was initially obtained from sample e.<sup>9</sup> We have already shown (see Figure 14) that after isothermal crystallization and cooling to room temperature this sample does not display any definite morphology, i.e., an “h”-type scattering pattern corresponding to an “h”-type morphology is observed. The SALS patterns show that after 36 h at 104.5 °C this fraction has not developed any definite morphology, although 11% crystallinity has been

attained. After this isothermal crystallization, the cooling to room temperature does not lead to any change in the basic light scattering pattern. Spherulites do not form in contrast to the results for the unfractionated polymer. An electron microscope study of this same sample crystallized at 105.3 °C for 6 days and then cooled to room temperature has confirmed that the structure grown at the high temperatures and those formed on cooling are randomly arranged lamellae.<sup>4</sup> It is possible to distinguish between the two different situations because the lamellae grown at the high temperature are thicker than those formed on cooling.

The results that have been presented so far indicate that unfractionated polymers as well as molecular weight fractions can develop nonspherulitic morphologies at the elevated temperatures. However, a comparison of the *in situ* studies of sample e at 106 °C with those of fraction B7 at 104.5 °C, the concentration of side-chain branches being identical in both samples, would indicate a greater tendency to grow nonspherulitic structures in the molecular weight fractions under these conditions. Thus the conclusions reached from the room-temperature studies are confirmed by those at the isothermal crystallization temperature.

One might postulate that the difference between fractions and whole polymers is that fractionation or molecular segregation occurs with the latter. The influence of molecular weight on the crystallization kinetics, as evidenced by the data in Figure 3 and described elsewhere for other systems,<sup>14,15</sup> makes this a tempting concept if individual chains actually crystallized independently of one another. Molecular weight fractionation, or chain segregation, has been postulated to occur during the crystallization of bulk-crystallized polyethylene.<sup>18,19</sup> Close scrutiny of careful experiments makes clear, however, that if segregation occurs upon crystallization, it only happens in the low molecular weight range,  $5 \times 10^3$  or less.<sup>20,21</sup> This explanation of the experimental results had been considered previously for the crystallization of an unfractionated polyethylene sample<sup>2</sup> corresponding to sample e in the present work. To check this hypothesis the low molecular weight, spherulite-forming portion was extracted from the sample. It was found, however, that the morphological form remained unaltered after isothermal crystallization and subsequent cooling to room temperature. To further investigate the possibility that some molecular weight species could crystallize preferentially at the elevated temperature and in some way favor spherulitic growth, a comparative study was made here of a fraction and whole linear polyethylene.

In order to simplify the interpretation of the results, two samples of comparable weight-average molecular weight were chosen. These were Marlex-50 ( $M_w \approx 1.7 \times 10^5$ ,  $M_w/M_n = 12.5$ ) and a fraction ( $M_w = 1.6 \times 10^5$ ,  $M_w/M_n = 1.11$ ). An important consideration in designing this set of experiments is the choice of the respective crystallization temperatures. They must be chosen so as to give comparable crystallization rates. In addition, for the success of the experiment both samples must yield spherulites when they are rapidly cooled and they should develop rodlike structures at the elevated temperatures. Figure 10 indicates that Marlex-50 can only develop rodlike structures over a very narrow range of crystallization temperatures. We chose a crystallization temperature of 129.8 °C for this sample. Comparable kinetics, as well as a rodlike morphology, are obtained at 131.8 °C for the fraction  $M_w = 1.6 \times 10^5$ .

The light scattering patterns obtained for the unfractionated Marlex-50 in this experiment are given in Figure

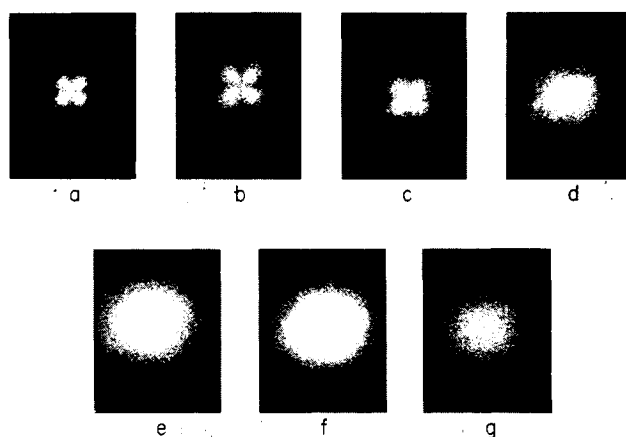


Figure 19.  $H_v$  SALS patterns for unfractionated linear polyethylene (Marlex 50) after initial partial crystallization at 129.8 °C and quenching into dry ice/2-propanol. Percent initial crystallization: pattern a, 0.0; pattern b, 0.2; pattern c, 3.0; pattern d, 7.0; pattern e, 15.0; pattern f, 38.0; pattern g, 63.0.

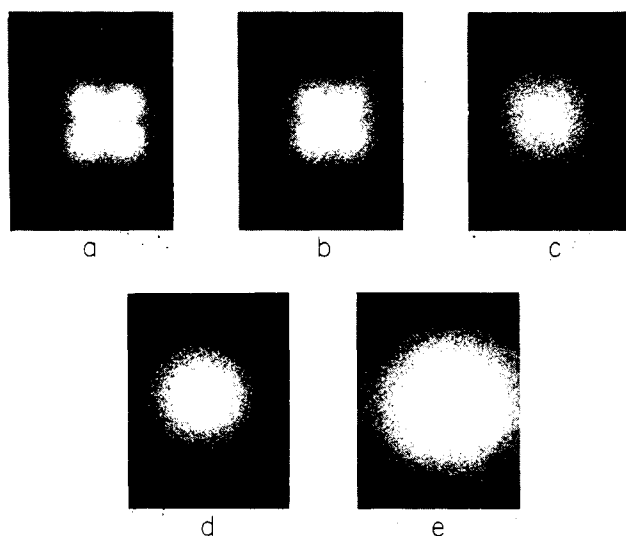
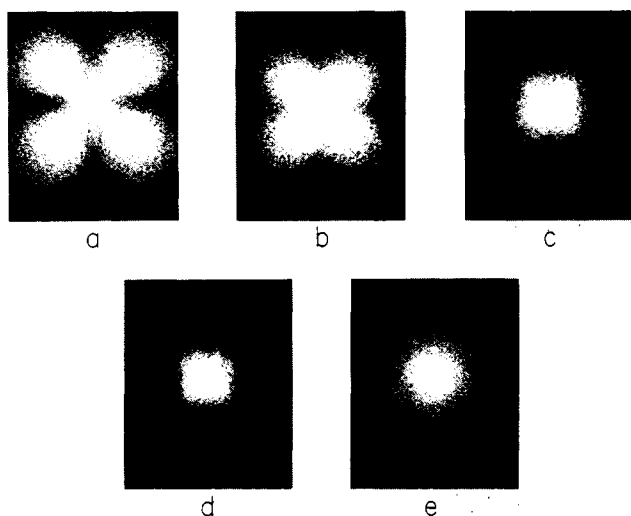


Figure 20.  $H_v$  SALS patterns for linear polyethylene fraction  $M_w = 1.6 \times 10^5$  after initial partial crystallization at 131.8 °C and quenched into dry ice/2-propanol. Percent initial crystallization: pattern a, trace; pattern b, 3.0; pattern c, 7.5; pattern d, 13.0; pattern e, 31.0.

19. The sample was allowed to crystallize a fixed amount and then the morphology was examined after quenching into dry ice/isopropyl alcohol. The reference pattern, quenching from the melt, i.e., no crystallinity at the elevated temperatures, is characteristic of well-developed spherulites. After 19 h, 0.2% crystallinity has developed and spherulitic structures are observed at room temperature. Three percent crystallinity has developed in 24.5 h, and spherulites are still observed. However, after 7% crystallinity has developed, in about 45 h, the spherulitic structures are no longer observed; the rodlike form is maintained. The development of successively larger amounts of isothermal crystallinity continues the trend of maintaining the rodlike structures. Thus, when about 7% rodlike crystallinity is developed at the elevated temperature, spherulitic growth is prevented upon cooling. Smaller amounts of this form, developed at the elevated temperature, do not have this property. Thus, the rodlike form directs the rest of the crystallization process.

The results of the same type of experiment with the molecular weight fraction are given in Figure 20. The reference structure is again that of a well-developed spherulite. Such structures are still observed when the



**Figure 21.**  $H_v$  SALS patterns for unfractionated, branched polyethylene sample a after initial isothermal crystallization at 117.5 °C and quenched into dry ice/2-propanol. Percent initial crystallization: pattern a, reference sample, 0.0; pattern b, 2.6; pattern c, 3.5; pattern d, 5.5; pattern e, 9.1.

initial, isothermal levels of crystallinity reach 3%, which takes approximately 45 h. However, when about 7% rodlike structures are initially developed, these structures are maintained upon subsequent cooling and further crystallization, i.e., the process of spherulite formation is arrested. Similar results are found with initial higher levels of crystallinity. Thus the linear fraction and unfractionated samples give essentially identical results. If molecular weight fractionation were taking place in the unfractionated sample as a consequence of isothermal crystallization, it would have been necessary to develop a significantly greater amount of rodlike entities than in the fraction in order to retard the development of spherulitic structures. The results are, however, identical. We must therefore conclude that molecular weight fractionation cannot be the cause of any differences found under these isothermal crystallization conditions.

The requirements enumerated above for this experiment make it virtually impossible to carry out a meaningful comparison between an unfractionated branched polyethylene sample and a fraction with a similar branching concentration, molecular weight, and crystallization kinetics. The main reasons for this restriction are the limited isothermal crystallization range and the amount of crystallinity that can be developed. However, similar kinds of information can be derived by recognizing from the SALS patterns of Figure 9 that sample a can develop a rodlike structure, with a significant amount of crystallinity, when isothermally crystallized at an elevated temperature. Figure 21 gives the light scattering pattern for this sample after isothermally crystallizing to a specific degree of crystallinity and then cooling. The isothermal crystallization temperature was chosen at 117.5 °C since rodlike structures are formed under these conditions. These light scattering patterns make clear that between 6 and 9% rodlike structures can prevent subsequent spherulite formation. Smaller amounts of the initial rodlike crystallinity allow for spherulites to develop, similar to the reference structure. Thus, there is a quantitative similarity to the results for the linear polymer. Although a direct com-

parison with a branched fraction cannot be made, these results, together with the extraction studies previously described,<sup>2</sup> make it highly unlikely that molecular fractionation plays any role in governing the morphological differences observed.

The experiments conducted under controlled isothermal crystallization conditions lead to the conclusion that if a spherulitic structure is initially formed isothermally, it will continue to develop on cooling. On the other hand, when rodlike structures (g morphology) are found, it is possible, within narrow limits, to arrest this mode of crystallization and produce spherulites on cooling. However, when the amount of crystallinity in rodlike form becomes about 7% or greater, crystallinity will continue to develop in this morphological mode when cooled. When dispersed throughout the system, small amounts of crystallinity in rodlike form act as seeds which direct the formation of spherulites when more rapid crystallization conditions are made available. These structures can be thought of as macroscopic-scale nuclei for spherulite formation. We can then anticipate that a wide range and control of spherulitic sizes can be obtained with this crystallization procedure with essentially the same level of crystallinity.

We have also found that whole polymers display a greater propensity to form spherulites after isothermal crystallization and cooling as compared to fractions with similar molecular weight and branching content. Molecular weight fractionation can be ruled out as being of any significance in this process. There would thus appear to be an inherent effect of the polydispersity on the morphology. This great sensitivity to polydispersity must be a reflection of the isothermal time course of the crystallization and the temperature interval, or undercooling, accessible to isothermal crystallization. Except for unduly long times, either spherulites form initially or the rodlike degree of crystallinity has not exceeded its critical value to form spherulitic nuclei.

**Acknowledgment.** Support of this work by Exxon Chemical Corp. is gratefully acknowledged.

## References and Notes

- Maxfield, J.; Mandelkern, L. *Macromolecules* **1977**, *10*, 1141.
- Mandelkern, L.; Maxfield, J. *J. Polym. Sci., Polym. Phys. Ed.* **1979**, *17*, 1913.
- Mandelkern, L. *Discuss. Faraday Soc.* **1979**, *68*, 310.
- Mandelkern, L.; Glotin, M.; Benson, R. A. *Macromolecules* **1981**, *14*, 22.
- Mandelkern, L.; Go, S.; Peiffer, D.; Stein, R. S. *J. Polym. Sci., Polym. Phys. Ed.* **1977**, *15*, 1189.
- Flory, P. J. *J. Chem. Phys.* **1949**, *17*, 223.
- Flory, P. J. *Trans. Faraday Soc.* **1955**, *51*, 845.
- Mandelkern, L. "Crystallization of Polymers"; McGraw-Hill: New York, 1964.
- Westerman, L.; Clark, J. C. *J. Polym. Sci., Polym. Phys. Ed.* **1973**, *11*, 559.
- Stein, R. S. "Structure and Properties of Polymer Film"; Lenz, R. W., Shaw, R. S., Eds.; Plenum: New York, 1972.
- Chiang, R.; Flory, P. J. *J. Am. Chem. Soc.* **1961**, *83*, 2057.
- Gornick, F.; Mandelkern, L. *J. Appl. Phys.* **1962**, *33*, 907.
- Hser, J. C.; Carr, S. H. *Polym. Eng. Sci.* **1979**, *19*, 436.
- Ergoz, E.; Fatou, J. G.; Mandelkern, L. *Macromolecules* **1972**, *5*, 147.
- Jadraque, D.; Fatou, J. M. G. *An. Quim.* **1977**, *73*, 639.
- Flory, P. J.; Vrij, A. *J. Am. Chem. Soc.* **1963**, *85*, 3548.
- Quinn, F. A.; Mandelkern, L. *J. Am. Chem. Soc.* **1958**, *80*, 3178.
- Mehta, A.; Wunderlich, B. *Colloid Polym. Sci.* **1975**, *253*, 193.
- Wunderlich, B. *Discuss. Faraday Soc.* **1979**, *68*, 239.
- Jackson, J. F.; Mandelkern, L. *Anal. Calorim.* **1968**, *1*, 1.
- Mandelkern, L. *Discuss. Faraday Soc.* **1979**, *68*, 414ff.